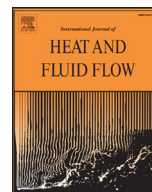




ELSEVIER

Contents lists available at ScienceDirect

International Journal of Heat and Fluid Flow

journal homepage: www.elsevier.com/locate/ijhff

Modeling of coherent structures in a turbulent jet as global linear instability wavepackets: Theory and experiment

Onofrio Semeraro^{a,*}, Lutz Lesshafft^a, Vincent Jaunet^b, Peter Jordan^b

^aLadHyX, CNRS, École polytechnique – Palaiseau, FR

^bInstitut PPRIME, CNRS, Université de Poitiers, ENSMA – Poitiers, FR

ARTICLE INFO

Article history:
Available online xxx

Keywords:
Turbulent jet
Frequency response analysis
Linear stability analysis
Aeroacoustics

ABSTRACT

Perturbation wavepackets in a jet, induced by externally applied forcing, are computed from the linearized equations of motion. An experimentally measured mean flow serves as the base state for this linear analysis, and optimally amplified mono-frequency perturbations are identified, in the sense of maximal gain between the forcing energy input and the flow response energy. Sub-optimal orthogonal forcing/response structures are also discussed. Linear analysis results are then compared to measured perturbation wavepackets in the jet experiment. The study addresses the question to what extent the true dynamics of a turbulent jet can be represented by a model based on linear instability.

© 2016 Elsevier Inc. All rights reserved.

1. Introduction

Since the experiments by Mollo-Christensen (Mollo-Christensen, 1963) and by Crow & Champagne (Crow and Champagne, 1971), it has been recognized that turbulent jets exhibit large-scale vortical structures of relatively high spatial and temporal coherence. These structures are well described as wavepackets of synchronized frequency, with streamwise amplitude and phase modulations. It has furthermore been established that the dominant noise radiated from such jets is correlated with these wavepacket structures, as for instance in the numerical study by Freund (Freund, 2001). Many investigations have since been based on the idea that the coherent wavepackets in turbulent jets and other shear flows may be modeled as instability waves (e.g. Cavalieri et al., 2013; Crighton and Gaster, 1976), linear or nonlinear, that develop in some steady state, either a laminar steady solution of the Navier–Stokes equations or an empirically determined mean flow. Such a model is tempting, because it opens a way for the analysis of the perturbation dynamics and, if the model carries that far, of the sound-producing mechanisms that are responsible for the jet noise.

However, the description of wavepackets in turbulent jets as instability waves within a steady flow state requires an empirical justification. A recent review (Jordan and Colonius, 2013) cites several studies that corroborate the pertinence of such an approach. In particular, Suzuki and Colonius (2006) present sophisticated exper-

imental measurements of near-field pressure fluctuations outside the shear layer of subsonic high Reynolds number jets, and they demonstrate that the coherent fluctuations compare well with the local k^+ instability mode characteristics. Cavalieri et al. (2012) take this approach further, by comparing PIV data obtained in the interior of a $Ma = 0.4$ jet with linear PSE instability calculations. Their study shows remarkable agreement in the development of vortical wavepackets throughout the potential core of the mean flow, for Strouhal numbers between 0.3 and 0.9. At lower Strouhal numbers, and at streamwise distances beyond the potential core, measurements and PSE predictions differ significantly.

The aim of this study is to extend the comparison between experiment and theoretical modeling to a framework of fully global linear stability analysis, named the linear frequency response. Optimization is performed in order to identify the most energy-efficient linear forcing of a jet at a given Strouhal number. New high-quality experimental data, obtained in a jet at $Ma = 0.9$ and $Re = 10^6$, is used for a detailed comparison between linear flow-response wavepackets and coherent turbulent structures. A similar investigation by Jeun et al. (2016) established good agreement between linear frequency response and LES results for a jet at nominally identical operating conditions. Linear frequency response analysis has been applied in earlier work (Garnaud et al., 2013a, 2013b) to different jet configurations. In the present paper, the formalism is applied for the first time to experimental jet data.

The paper is organized as follows. The experimental setup is described in Section 2; mean flow quantities are shown, and the main frequency-resolved PIV results are summarized. The frequency response analysis, and some details on numerical procedures, are presented in Section 3. Linear analysis results are

* Corresponding author.

E-mail address: semeraro@ladhyx.polytechnique.fr (O. Semeraro).

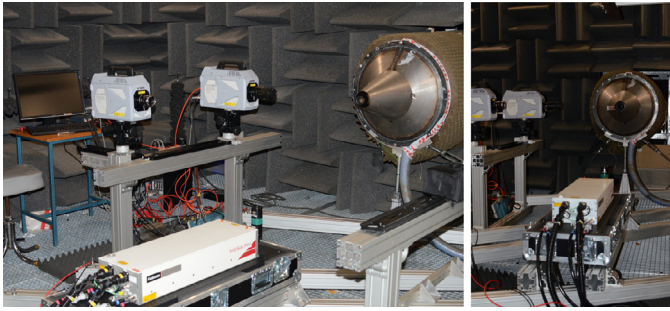


Fig. 1. The "Bruit et Vent" experimental set-up.

documented in Section 4 and compared to experimental data in Section 5.

2. Experimental setup

Experiments were conducted at the "Bruit et Vent" jet-noise facility at the CEAT, PPRIME Institute, Poitiers, France. The measurements were carried out at a Mach number ($Ma = U_j/c$, where U_j is the jet velocity and c the ambient speed of sound) equal to 0.9 in isothermal conditions. The nozzle diameter D was 0.05 m, giving a Reynolds number of $Re_D = \rho U_j D / \mu \approx 10^6$. Transition in the incoming internal boundary layer is triggered using a Carborundum strip glued on the wall upstream from the nozzle exit.

The PIV system consisted of a Photron SAZ camera and a 532 nm Continuum MESA PIV laser providing 6 mJ of light pulse energy. The system was placed on a traverse parallel to the jet axis in order to scan the jet flow field from axis location close to the nozzle up to 20 jet diameter. The camera was equipped with a 100 mm macro lens with low optical distortion, the aperture set at f#4. A photograph of the set-up is given in Fig. 1.

Two different field of views (FOV) were used during the experimental campaign. The first FOV measured the velocity field in an area of about $2D \times 2D$, and was used for axial positions from the nozzle exit up to $x = 6D$. The second FOV measured the velocity field in an area of $4D \times 4D$, and was used for more downstream locations, i.e. $x > 5D$. Hence, a finer spatial resolution was obtained for measurements close to the nozzle exit to ensure a good capture of the local velocity gradients. The complete measurement of the jet flow was obtained with the use of 11 ac-

quisitions performed at various downstream locations. In between each of these locations an overlap of 20% of the FOV was set in order to control the correct alignment of the measured velocity fields. A calibration was made at all acquisition positions in order to be able to correct for both the remaining optical distortions and laser light sheet/measurement plane misalignment using a self-calibration procedure (Wieneke, 2005).

Both the jet flow and the surrounding air were seeded using glycerin smoke particles, whose diameter lays in the range between 1 and 2 μm , thus sufficiently small to follow the velocity fluctuations of interest in this paper. The particles formed images of 2–3 particles in diameter, and no evidence of peak-locking was found in the data set.

The image acquisition was performed at 20 kHz (10,000 PIV samples a second) at a resolution of 1024×1024 pixels. The time between the two laser pulses was set according to the local velocity amplitude and to the laser sheet width (which was set at 2 mm), and ranged between 4 and 5 μs . For each acquisition 42,000 image pairs were acquired.

PIV calculations were carried out using a commercial software, and a multi-pass iterative PIV algorithm with deforming interrogation area (Scarano, 2002) to account for the local mean velocity gradients. The PIV interrogation area size was set to 32×32 pixels for the first pass, decreased at 16×16 pixels for the remaining passes, with an overlap of 50% between two neighboring interrogation areas. Displacement computed were retained only the correlation peak-ratio was higher than 1.3. After each pass a Universal Outlier Detection (UOD) (Westerweel and Scarano, 2005) is applied on a 3×3 vector grid to avoid corrupted data and enhance the particle motion calculation. Finally, prior to the computation of the flow statistical quantities a 5-sigma filter is applied to remove the remaining outliers and they are replaced using the UOD technique.

2.1. Mean flow measurements and postprocessing

The mean flow for which all further analysis will be performed is computed from the PIV measurements through time-averaging. The axial velocity component \bar{u} is presented in Fig. 2a, and the correlation $\overline{u'v'}$ of velocity fluctuations around the mean flow, from which the turbulent viscosity will be estimated, is shown in Fig. 2b. The potential core extends about six diameters downstream of the nozzle exit.

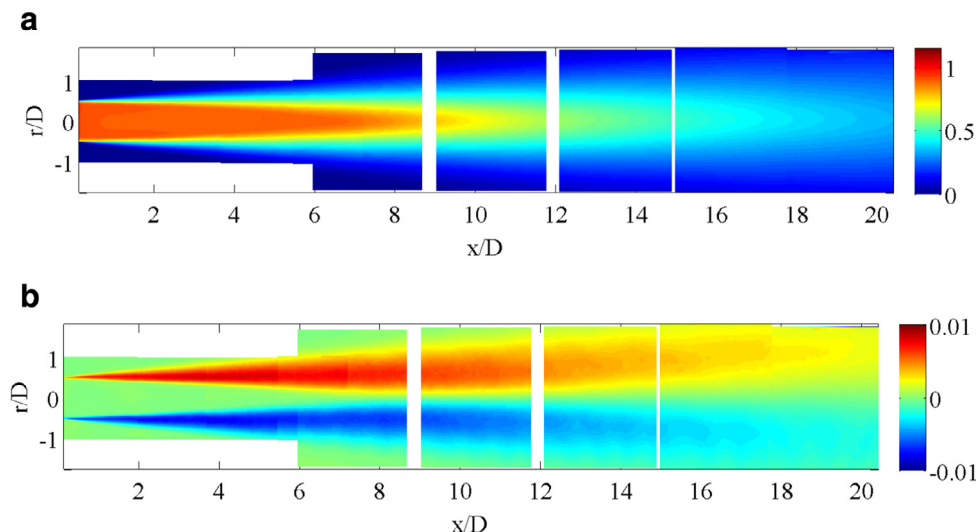


Fig. 2. PIV results: the spatial distribution of the meanflow axial velocity and the $\overline{u'v'}$ fluctuations are shown in (a) and (b), respectively.

Download English Version:

<https://daneshyari.com/en/article/4993319>

Download Persian Version:

<https://daneshyari.com/article/4993319>

[Daneshyari.com](https://daneshyari.com)